Journal of Applied Mechanics and Technical Physics, Vol. 45, No. 6, pp. 853–859, 2004

TWO NONLINEAR MODELS OF BRITTLE FRACTURE FOR SOLIDS

A. V. Shutov

UDC 518.61: 539.375

This paper considers isotropic and orthotropic nonlinear constitutive relations for brittle materials in the case of plane stresses. Numerical solution algorithms based on the finite-element method are developed. The resulting material models are incorporated in the PIONER software. The correctness of crack path determination is examined by solving a test problem of crack propagation. The isotropic model gives mesh-dependent results, whereas the orthotropic model provides an adequate solution. It is shown that solutions obtained for the isotropic model are close to those obtained by eliminating failed elements.

Key words: *mechanics of deformable solids, finite-element method, fracture mechanics, brittle fracture.*

Introduction. Numerical modeling of crack nucleation and propagation began in the late 1960s and is dealt with in fundamental papers [1, 2], where the so-called "discrete" and "smeared" crack models are introduced. With time, the second approach based on models of the second type has gained popularity. It consists of modeling a crack within the framework of continuum mechanics by introducing nonlinear constitutive relations of the material. This is equivalent to introducing physical nonlinearity. A review and classification of the models is given in [3].

The most appropriate method for the numerical solution of nonlinear problems of solid-state mechanics is the finite-element method (FEM). It underlies the development of a technology for solving nonlinear problems of solid-state mechanics [4–6], in particular, nonlinear fracture mechanics. Problems of nonlinear fracture mechanics can be considered as a particular case of elastoplastic problems (material behavior does not depend explicitly on time) with constitutive relations of special form.

A distinctive feature of these problems is the absence of a theorem on the existence and uniqueness of solutions. Under such conditions, in general, a numerical solution may not converge to the exact solution and does not depend continuously on the input data. Success of using each particular nonlinear model depends on many factors: its adequacy to the physics of the phenomenon, logical simplicity, and the existence of an effective and stable procedure for numerical integration.

The subject of the present study is the correctness of modeling solid fracture, in particular, crack nucleation and propagation in a brittle isotropic material using the FEM. Here, the FEM is considered as a version of the Bubnov–Galerkin method with the basis functions defined in local subdomains (finite elements).

The paper gives a general formulation of the problem of nonlinear solid-state mechanics. Constitutive relations are formulated for two models of a brittle material. In both models, the deformation is assumed to be elastic up to fracture and fracture occurs when the principal tensile stress exceeds the ultimate strength of the material. In the isotropic model, the material fails instantaneously and completely upon fracture, and in the orthotropic model, the fractured material can be modeled by an orthotropic material weakened in a certain direction. The latter is a particular case of the model proposed and successfully used in [7].

Lavrent'ev Institute of Hydrodynamics, Siberian Division, Russian Academy of Sciences, Novosibirsk 630090; shutov@ngs.ru. Translated from Prikladnaya Mekhanika i Tekhnicheskaya Fizika, Vol. 45, No. 6, pp. 95–102, November–December, 2004. Original article submitted October 1, 2003; revision submitted December 1, 2003.

The isotropic and orthotropic models are studied by solving a test problem of crack nucleation and propagation. In spite of the fact that the exact solutions of this test problem obtained for the two constitutive relations are equal, the numerical solutions differ considerably. The isotropic model fails to predict the cracking pattern adequately. The orthotropic model has advantages over the isotropic model in this respect.

The method of elimination of failed elements has bee widely used recently. In this method, elements in which fracture occurs are eliminated from the element assemblage. This method is a formal simplification of the method based on the isotropic model. Numerical experiments have shown that these methods give close results. As in case of the isotropic model, the method of eliminated elements fails to predict the crack pattern.

1. Equations of Solid-State Mechanics Taking into Account Physically Nonlinearity and Their Spatial Discretization. Formulations of the basic equations and their discrete analogs for nonlinear problems of solid-state mechanics can be found, for example, in [4–6]. We give equations that describe deformations of a solid body under the assumption of small strains, rotations, and displacements (at the same time, large rigid-body translation motion is allowed).

Let t be a monotonically increasing deformation parameter. In quasistatic problems, by the parameter t is meant, as a rule, the external force, prescribed displacement, arc length of the integral curve in the displacement-load space, etc. The basic equations of the problem taking into account physical nonlinearity are given below. 1. Equations of equilibrium

$$\boldsymbol{\nabla} \cdot \sigma = \mathbf{0} \qquad \text{in} \quad V \tag{1}$$

with the boundary and initial conditions

$$\boldsymbol{u} = \boldsymbol{u}^* \quad \text{on} \quad S_u, \qquad \boldsymbol{N} \cdot \sigma = \boldsymbol{T}^* \quad \text{on} \quad S_T, \qquad \boldsymbol{u}\Big|_{t=0} = \boldsymbol{u}_0.$$

Here and below, σ is the Cauchy stress tensor, $\boldsymbol{u}$ is the displacement tensor, V is the region occupied by the body in the initial state, S is the closed surface bounding V, S_u and S_T are the parts of the surface $S = S_u \cup S_T$ on which the displacement and stress vectors $\boldsymbol{u}$ and $\boldsymbol{T} \equiv \boldsymbol{N} \cdot \sigma$, respectively, are specified, $\boldsymbol{N}$ is the outward unit normal vector to the surface S_T, and $\boldsymbol{u}_0$ is the initial-displacement vector; the specified quantities are marked by an asterisk.

2. Kinematic relations

$$\varepsilon = (\boldsymbol{\nabla}\boldsymbol{u} + \boldsymbol{\nabla}\boldsymbol{u}^{\mathrm{t}})/2,$$

where ε is the Cauchy strain tensor and $\boldsymbol{\nabla}\boldsymbol{u}$ is the displacement gradient tensor.

3. Constitutive relation (at each material point)

$$\dot{\sigma} = C : \dot{\varepsilon}, \tag{2}$$

where C is a fourth-rank tensor, whose components generally depend on the deformation history and the dot above denotes differentiation with respect to the deformation parameter t.

We consider the weak form of the equations of motion (1) expressed by the equation of the possible displacement principle

$$\int\limits_V \sigma : \delta\varepsilon \, dV = \int\limits_{S_T} \boldsymbol{T}^* \cdot \delta\boldsymbol{u} \, dS \qquad \forall\, \delta\boldsymbol{u}. \tag{3}$$

where δ denotes variation such that $\delta\boldsymbol{u} = \mathbf{0}$ on S_u (the boundary conditions on S_u are principal and those on S_T are natural) and the Cauchy strain tensor variation is given by

$$\delta\varepsilon = [\boldsymbol{\nabla}(\delta\boldsymbol{u}) + \boldsymbol{\nabla}(\delta\boldsymbol{u})^{\mathrm{t}}]/2.$$

Let us consider the case of plane stresses assuming that

$$\sigma_{33} = \sigma_{13} = \sigma_{23} = 0, \qquad T_3^* = 0. \tag{4}$$

The discrete analog of the equilibrium equations is obtained using the FEM based on the equilibrium equations written in the weak form (3). We consider isoparametric finite elements for which the radius-vectors of the material points and the displacement vector are approximated by the same set of polynomials. We consider the mth finite element and introduce the vectors

$$\boldsymbol{\sigma} = [\sigma_{11}, \sigma_{22}, \sigma_{12}]^{\mathrm{t}}, \qquad \boldsymbol{\varepsilon} = [\varepsilon_{11}, \varepsilon_{22}, 2\varepsilon_{12}]^{\mathrm{t}},$$

and the nodal displacement vector of the element

$$\boldsymbol{U}^m = [u_1^1, u_2^1, \dots, u_1^N, u_2^N]^{\mathrm{t}},$$

where u_i^k is the ith component of the displacement vector at the kth nodal point of the element. The constitutive relations (2) can be written in matrix form

$$\dot{\boldsymbol{\sigma}} = C\dot{\boldsymbol{\varepsilon}}, \tag{5}$$

where C is a 3×3 symmetric matrix whose elements consist of the components of the corresponding fourth-rank tensor under hypothesis (4). Let $\boldsymbol{u} = (u_1, u_2)$. We introduce the matrices B and H of an element such that the following relations are satisfied in the mth element:

$$\boldsymbol{\varepsilon} = B\boldsymbol{U}^m, \qquad \boldsymbol{u} = H\boldsymbol{U}^m.$$

The matrices B and H depend only on the geometry of the element and remain unchanged during its deformation. We introduce the tangential stiffness matrix of the element (K^m), the surface-force vector of the element ($\boldsymbol{R}^m$), and the internal-force vector of the element ($\boldsymbol{F}^m$):

$$K^m \equiv \int\limits_{V^m} B^{\mathrm{t}} C B \, dV, \qquad \boldsymbol{R}^m \equiv \int\limits_{S_T^m} H^{\mathrm{t}} \boldsymbol{T}^* \, dS, \qquad \boldsymbol{F}^m \equiv \int\limits_{V^m} B^{\mathrm{t}} \boldsymbol{\sigma} \, dV. \tag{6}$$

The integrals in (6) are calculated using the Gauss–Legendre quadrature formulas.

We introduce the vector of the global degrees of freedom of the finite-element assemblage

$$\boldsymbol{U} = [U_1, U_2, \dots, U_{N_{EQ}}]^{\mathrm{t}},$$

where U_i ($i = \overline{1, N_{EQ}}$) is one of the components of the displacement vector at a certain nodal point and N_{EQ} is the total number of independent components of the displacement vector of the assemblage of the nodal points. For each mth element, the components of the vector $\boldsymbol{U}^m$ consist of the components of the global vector $\boldsymbol{U}$. The vectors $\boldsymbol{U}^m$, $\boldsymbol{R}^m$, and $\boldsymbol{F}^m$ and matrix K^m of each element are reduced to the size N_{EQ} and $N_{EQ} \times N_{EQ}$, respectively, using Boolean matrices A^m (whose elements consists of zeroes or unities) which are defined for the mth element by the relation

$$\boldsymbol{U}^m = A^m \boldsymbol{U}.$$

The global tangential stiffness matrix K and the external and internal force vectors ($\boldsymbol{R}$ and $\boldsymbol{F}$, respectively) of the finite-element assemblage are given by

$$K \equiv \sum_{m=1}^{M} A^{m\mathrm{t}} K^m, \qquad \boldsymbol{R} \equiv \sum_{m=1}^{M} A^{m\mathrm{t}} \boldsymbol{R}^m, \qquad \boldsymbol{F} \equiv \sum_{m=1}^{M} A^{m\mathrm{t}} \boldsymbol{F}^m, \tag{7}$$

where M is the total number of elements.

Then, the discrete analog of Eqs. (3) becomes

$$\delta\boldsymbol{U}^{\mathrm{t}}\boldsymbol{F} = \delta\boldsymbol{U}^{\mathrm{t}}\boldsymbol{R}. \tag{8}$$

By virtue of arbitrariness of the vector $\delta\boldsymbol{U}$, from (8) we obtain the discrete analog of the equilibrium equations — the system of nonlinear equations for $\boldsymbol{U}(t)$:

$$\boldsymbol{F}(t) = \boldsymbol{R}(t). \tag{9}$$

The equilibrium equations (9) are integrated by a step-by-step procedure. The deformation process is divided into N steps $[0, t_1), [t_1, t_2), \dots, [t_{N-1}, t_N)$, for each of which a solution $\boldsymbol{U}(t_i)$ is found. The dependence of the vector $\boldsymbol{F}(t)$ on the deformation history is taken into account as follows. It is assumed that the vector $\boldsymbol{F}(t_i)$ is uniquely determined by the sequence of states $\boldsymbol{U}(0), \boldsymbol{U}(t_1), \dots, \boldsymbol{U}(t_{i-1})$, and $\boldsymbol{U}(t_i)$. Fixing the solutions constructed at the previous steps, we assume that $\boldsymbol{F}(t_i) = \boldsymbol{F}(t_i, \boldsymbol{U}(t_i))$. The value of $\boldsymbol{U}(t_i)$ is obtained by solving the nonlinear system (9) using the iterative Newton method [4–6]. In the Newton method, the initial approximation is the solution $\boldsymbol{U}(t_{i-1})$ obtained at the previous time step. In each iteration, one needs to invert the tangential stiffness matrix $K(t_i)$, which is the Jacobi matrix for the function $\boldsymbol{F}(t_i, \boldsymbol{U})$. The algorithm for determining the function $\boldsymbol{F}(t_i, \boldsymbol{U})$ and the tangential stiffness matrix is specified by the particular model of the material.

2. Nonlinear Constitutive Relations for a Brittle Material. The constitutive relations (5) can be used to model brittle fracture of materials. We describe two versions of these relations for a brittle material assuming that plane stresses occur at the material point considered. To construct the vector $\boldsymbol{F}$ and the matrix K, it is necessary to perform numerical integration of the expressions in (6). To this end, the integrands are calculated at each integration point of the Gauss–Legendre formula. That is, one should determine C and $\boldsymbol{\sigma}$ at each integration point.

For the models considered in the present paper, material behavior is determined by three parameters: Young's modulus E, Poisson's ratio ν, and ultimate strength σ_t.

2.1. *Isotropic Model of a Brittle Material.* It is assumed that at each material point (integration point), the material exists in two states: the intact state and the complete failure state.

1. The intact state is modeled by a linear elastic isotropic material:

$$C = \frac{E}{1-\nu^2}\begin{bmatrix} 1 & \nu & 0 \\ \nu & 1 & 0 \\ 0 & 0 & (1-\nu)/2 \end{bmatrix}, \qquad \boldsymbol{\sigma} = C\boldsymbol{\varepsilon}. \tag{10}$$

2. The complete failure state is modeled by a material which has no carrying capacity

$$C = \frac{E}{1-\nu^2}\begin{bmatrix} k_1 & \nu k_1 & 0 \\ \nu k_1 & k_1 & 0 \\ 0 & 0 & (1-\nu)k_2/2 \end{bmatrix}, \qquad \boldsymbol{\sigma} = \mathbf{0}. \tag{11}$$

Here k_1 and k_2 are small positive numbers used to regularize the tangential stiffness matrix.

At the initial time, the material is intact. Transition from the first state to the second state occurs when the principal tensile stress exceeds the ultimate tensile strength.

2.2. *Orthotropic Model of a Brittle Material.* The orthotropic model is a particular case of the model given in [7] (which allows one to analyze brittle fracture of thin-walled structures). At each point, the material can exist in four states: the intact state, the open-crack state, the closed-crack state, and the complete failure state.

1. The intact state is modeled by a linear elastic isotropic material (10).

2. The open-crack state is modeled by a linear elastic orthotropic material weakened in a direction normal to the crack plane. In the principal axes of the stress tensor, the matrix of the constitutive relations and the stress vector are written as

$$\begin{gathered} \check{C} = \frac{E}{1-\nu^2}\begin{bmatrix} k_1 & \nu k_1 & 0 \\ \nu k_1 & 1 & 0 \\ 0 & 0 & (1-\nu)k_2/2 \end{bmatrix}, \\ \check{\sigma}_1 = \check{\sigma}_{12} = 0, \qquad \check{\sigma}_2 = \frac{E}{1-\nu^2}\,(\nu\check{\varepsilon}_{11} + \check{\varepsilon}_{22}). \end{gathered} \tag{12}$$

3. The closed-crack state is modeled by a linear elastic isotropic material (10), as in the case of the intact state.

4. The complete failure state is modeled by a material which has no carrying capacity (11).

Transition from the first to the second state occurs when the principal tensile stress exceeds the ultimate tensile strength under the assumption that the crack plane is normal to the first principal direction. Transition from the second to the third state occurs if the strain along the axis normal to the crack plane becomes negative. Transition from the third to the second state occurs if this strain is positive. If both principal stresses exceed the ultimate strength, the fourth state is attained. It is assumed that when being in the state of complete failure, the material cannot restore its carrying capacity.

3. Comparison of the Models by Solving the Failure Problem of a Symmetric V-Notched Specimen. The material models proposed were incorporated in the PIONER software [8]. The numerical solutions considered in this section were obtained using this software. Let us consider the failure of a V-notched brittle plate. Figure 1 shows the geometry of the plate. The lower end of the plate is clamped and the upper end is displaced as a rigid body by amount u in the vertical direction. The displacement of the end u is used as the

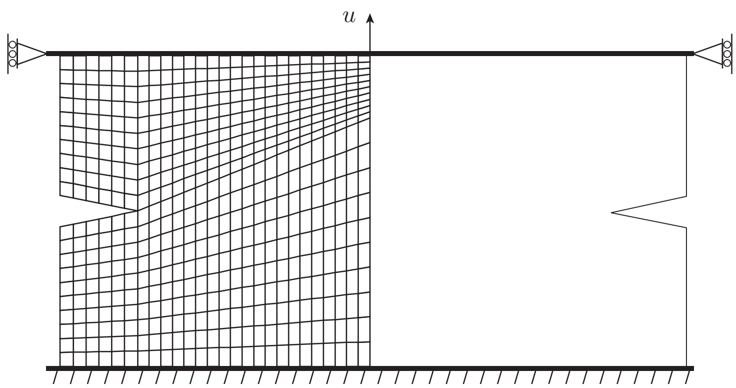

Fig. 1. Fracture of a V-notched plate: geometry and finite-element mesh.

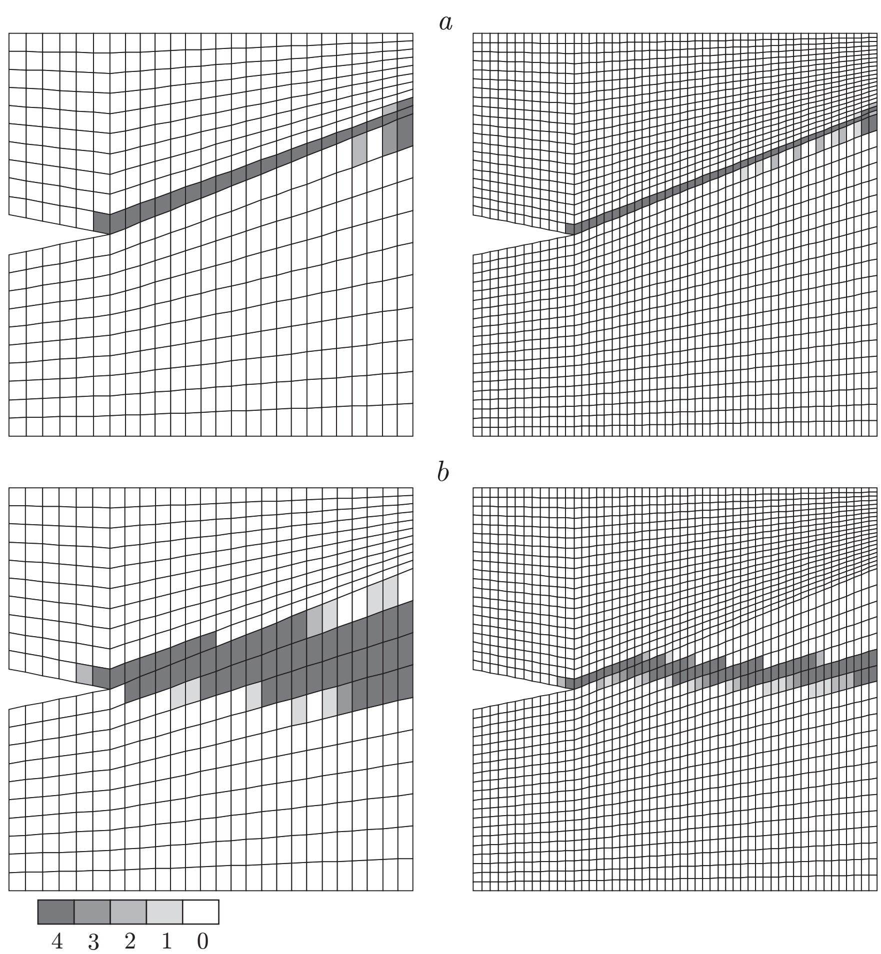

Fig. 2. Numerical solution of the problem for the isotropic model (a) and orthotropic model (b).

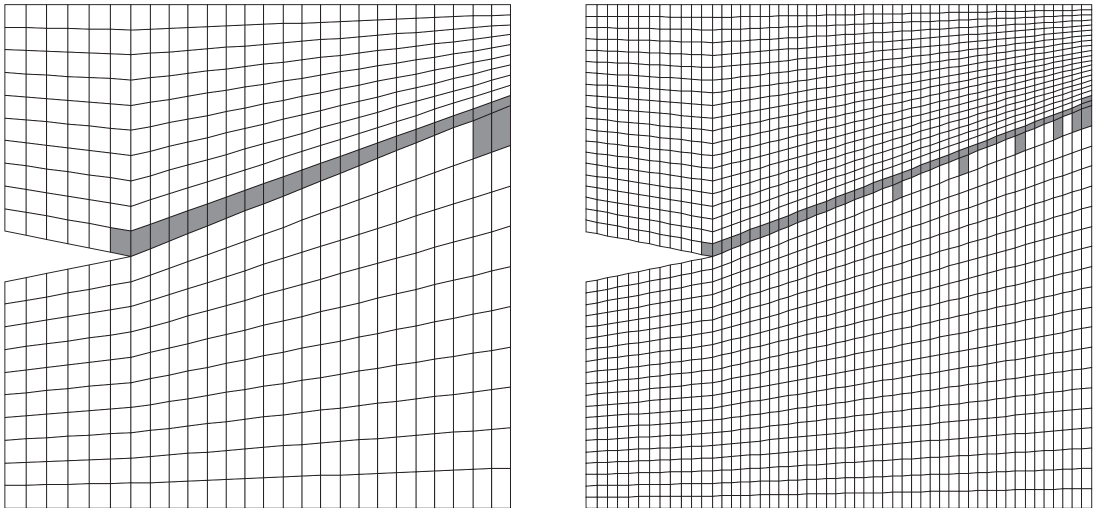

Fig. 3. Solution obtained by the procedure of eliminating failed elements

deformation parameter. Thus, we have the quasistatic problem that models the fracture of the plate under rigid loading. The calculation parameters were as follows: Young's modulus $E = 10^7$ Pa, Poisson's ratio $\nu = 0.25$, and ultimate strength $\sigma_t = 2 \cdot 10^4$ Pa. By virtue of the vertical and horizontal symmetry of the specimen, a crack should appear at the notch tip and propagate strictly in the horizontal direction for both models of the material. Owing to the vertical symmetry, only the left part of the plate was considered. In the calculations, elements with a linear approximation of the geometry and displacement vector were used. Numerical integration was performed by the Gauss–Legendre formulas with a total order of numerical integration of 2×2. All calculations were performed using a special finite-element mesh (see Fig. 1). In the vicinity of the notch tip, the mesh is oriented at an angle to the principal directions of the stress tensor. The calculation results for the isotropic and orthotropic models with varying finite-element partitioning are given in Figs. 2a and 2b, respectively. In Fig. 2, each elements is colored in accordance with the number of integration points at which failure (partial or complete) occurs. The maximum number of integration points is equal to four.

One can see from Fig. 2 that the isotropic model fails to predict the crack propagation direction adequately. The crack path depends on the mesh orientation. For the orthotropic model, the situation is different. As the mesh is refined, the crack path approaches a horizontal line and does not depend on the mesh orientation.

We note that the algorithm based on the isotropic model can be simplified as follows. Let us consider the computational scheme which uses only the linear elastic material model. If the failure criterion is satisfied in a certain element, this element is eliminated from the element assemblage. This is equivalent to eliminating the corresponding terms in formulas (7). The calculation results obtained by this scheme are given in Fig. 3. Unlike in the scheme based on the isotropic model, in the scheme considered, material failure occurs at once over the entire element rather than at a certain integration point. In Fig. 3, the eliminated elements are colored black. One can see that the solution is close to that obtained for the isotropic model. As for the isotropic model, the crack path does not approach a horizontal line as the mesh is refined.

Conclusions. Although the two models considered in this paper describe the same material behavior, these models differ from a computational viewpoint. The numerical schemes constructed for these models using the standard FEM procedure give significantly different results. For numerical schemes of this class, a condition for an adequate prediction of the crack growth direction is a good approximation of the stress field in the vicinity of the crack tip. The isotropic model and method of eliminated elements fail to satisfy this criterion, whereas the orthotropic model gives realistic results.

This work was supported by the Russian Foundation for Basic Research (Grant No. 02-01-00195), President of Russian Federation (Grant No. NSh-319.2003.1), and Ministry of Education of Russian Federation (Grant No. A03-2.10-617).

REFERENCES

1. Y. R. Rashid, "Analysis of prestressed concrete pressure vessels," *Nucl. Eng. Des.*, **7**, 334–344 (1968).
2. D. Ngo and A. C. Scordelis, "Finite element analysis of reinforced concrete beams," *J. Amer. Concr. Inst.*, **64**, 152–163 (1967).
3. R. De Borst, "Fracture in quasi-brittle materials: A review of continuum damage-based approaches," *Eng. Fract. Mech.*, **69**, 95–112 (2002).
4. K.-J. Bathe, *Finite Element Procedures in Engineering Analysis*, Englewood Cliffs, New Jersey, Prentice Hall (1982).
5. O. C. Zienkiewicz and R. L. Taylor, *The Finite Element Method*, London, McGraw Hill (1991).
6. S. N. Korobeinikov, *Nonlinear Deformation of Solids* [in Russian], Izd. Sib. Otd. Ross. Akad. Nauk, Novosibirsk (2000).
7. S. N. Korobeinikov, Yu. S. Khudyakov, and A. V. Shutov, "Mathematical modeling of brittle fracture of thin bodies," *Vychisl. Metod. Program.*, **3**, No. 2, 94–117 (2002).
8. S. N. Korobeinikov, V. P. Agapov, M. I. Bondarenko, and A. N. Soldatkin, "The general-purpose nonlinear finite element structural analysis program PIONER," in: *Proc. Int. Conf. on Numerical Methods and Applications* (Sofia, Bulgaria, August 22–27, 1989), Sofia (1989), pp. 228–233.